ACSNANO
www.acsnano.org
ARTICLE

Excluding Contact Electrification in Surface Potential Measurement Using Kelvin Probe Force Microscopy

Shengming Li,[†,‡,⊥] Yusheng Zhou,[†,⊥] Yunlong Zi,[†] Gong Zhang,[‡] and Zhong Lin Wang*[,†,§]

[†]School of Materials Science and Engineering, Georgia Institute of Technology, Atlanta, Georgia 30332-0245, United States
[‡]Department of Mechanical Engineering, Tsinghua University, Beijing 100084, China
[§]Beijing Institute of Nanoenergy and Nanosystems, Chinese Academy of Sciences, Beijing 100083, China

Supporting Information

ABSTRACT: Kelvin probe force microscopy (KPFM), a characterization method that could image surface potentials of materials at the nanoscale, has extensive applications in characterizing the electric and electronic properties of metal, semiconductor, and insulator materials. However, it requires deep understanding of the physics of the measuring process and being able to rule out factors that may cause artifacts to obtain accurate results. In the most commonly used dual-pass KPFM, the probe works in tapping mode to obtain surface topography information in a first pass before lifting to a certain height to measure the surface potential. In this paper, we have demonstrated that the tapping-mode topography scan pass during the typical dual-pass KPFM measurement may trigger contact electrification between the probe and the sample, which leads to a charged sample surface and thus can introduce a significant error to the surface potential measurement. Contact electrification will happen when the probe enters into the repulsive force regime of a tip−sample interaction, and this can be detected by the phase shift of the probe vibration. In addition, the influences of scanning parameters, sample properties, and the probe's attributes have also been examined, in which lower free cantilever vibration amplitude, larger adhesion between the probe tip and the sample, and lower cantilever spring constant of the probe are less likely to trigger contact electrification. Finally, we have put forward a guideline to rationally decouple contact electrification from the surface potential measurement. They are decreasing the free amplitude, increasing the set-point amplitude, and using probes with a lower spring constant.

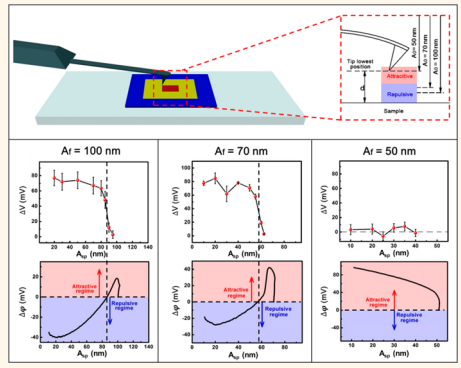

KEYWORDS: *surface potential measurement, dual-pass KPFM, contact electrification, tip−sample interactive force, phase shift change*

With the advances in nanoscience and nanotechnology, atomic force microscopy (AFM) has been developed with new applications to characterize a variety of material properties.[1−9] Among them, Kelvin probe force microscopy (KPFM), which is based on ascertaining the potential difference between the probe tip and the sample,[10] has been utilized to quantify the work function of a material.[11−14] It is not only important for comparing electric properties between different materials and describing the transport behavior of electronic devices and integrated circuits[15−18] but also powerful for probing the triboelectrification and contact electrification at the nanoscale.[19−21] For KPFM, a potential feedback loop and the corresponding DC voltage is applied between the tip and the sample to nullify the oscillation caused by the potential difference between the tip and sample.[22] Over the past decades, KPFM has been developed into two basic modes, the single-pass mode[23−27] and the dual-pass mode.[28−30] A single-pass scan acquires topographical and surface potential difference images simultaneously, while a dual-pass scan utilizes two passes to realize the topographical and surface potential scan separately. There is the cross-talk between topographical and surface potential images during single-pass measurement, and it requires proper parameter adjustment to minimize the cross-talk. In order to not obtain the lateral resolution restricted by the cross-talk, Stemmer *et al.* introduced the setup to do topography and potential measurements sequentially by implementing the lift-mode technique into a commercial AFM system.[29] Until now, the most commonly used scanning mechanism for KPFM is the dual-pass mode,[24] with general researchers restricted to commercial dual-pass KPFM setups that cannot be altered. Therefore, it is extremely necessary to rule out the possible

Received: November 24, 2015
Accepted: January 29, 2016

DOI: 10.1021/acsnano.5b07418
ACS Nano XXXX, XXX, XXX−XXX

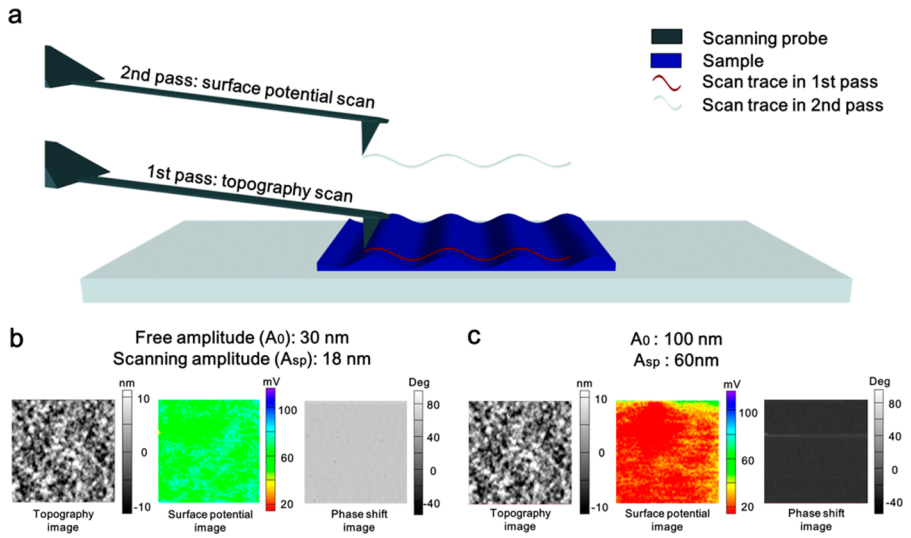

Figure 1. Scanning process of the KPFM measurement with two groups of scan results. (a) Schematic of the two-pass KPFM measurement with a figure legend in the inset. (b) Results of topography, surface potential, and phase shift measurements with A_0 = 30 nm and A_{sp} = 18 nm. (c) Results of topography, surface potential, and phase measurement with A_0 = 100 nm and A_{sp} = 60 nm.

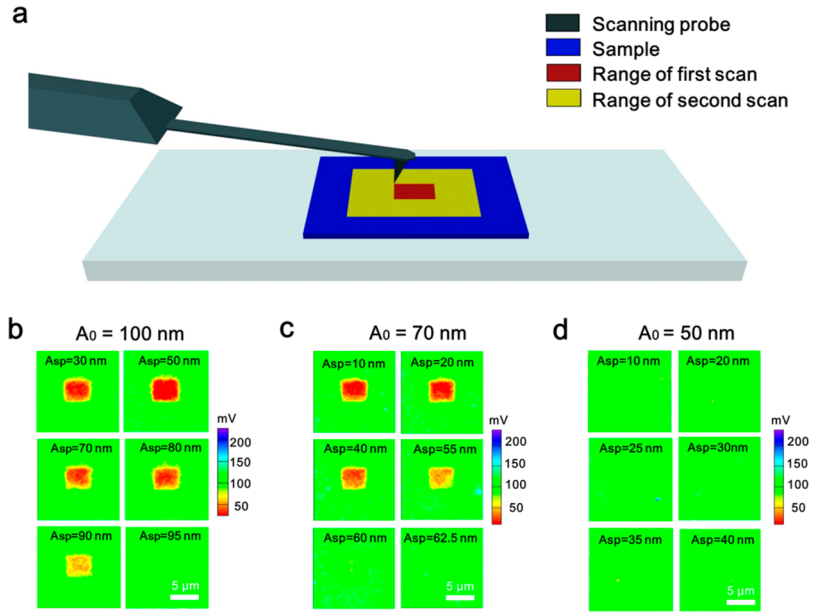

Figure 2. Two-time scanning experiment to explore the relationship between contact electrification and scanning parameters (A_0 and A_{sp}). (a) Schematic of the two-time scanning method with a figure legend in the inset. (b–d) Surface potential distribution after the second KPFM scan (~16 μm^2 in area) with the scanning parameters of A_0 = 100, 70, and 50 nm with different A_{sp} in the first scan, respectively.

factors and errors that may affect the accuracy and reliability of dual-pass KPFM. As shown in Figure 1a, a typical dual-pass KPFM measurement proceeds with two passes in one scan line.[9] The first pass is a topography scan in the tapping mode, with the aim to determine the topography of the sample surface and to eliminate the inaccuracy of the measurement caused by the change of the tip–sample distance. The second pass is the tip–sample potential difference measurement. During this pass, the tip is raised by a certain distance above the surface. Meanwhile, the potential feedback loop is implemented onto the tip–sample system to realize the surface potential measurement. In order to improve the accuracy of the measurement, researchers have been working on the capacitive effect associated with the cantilever in the second pass.[22] However, the influence of the topography scan, mainly in the way of contact electrification between the probe tip and the sample during the tapping process, has long been ignored, which, however, is particularly crucial for the measurement of insulator and semiconductor materials.

In this paper, we have demonstrated the existence of contact electrification during the surface potential measurement of KPFM for insulator and semiconductor materials. It has been proven that only in the condition that the probe tip enters into the repulsive regime of the tip–sample interaction force, there is significant surface potential change caused by contact electrification between the tip and the sample. Moreover, whether the tip is in the attractive regime or repulsive regime above the surface of the sample could be known from the change of the phase shift ($\Delta\varphi$) during the tapping vibration. In this way, we can predict whether there is contact electrification

DOI: 10.1021/acsnano.5b07418
ACS Nano XXXX, XXX, XXX–XXX

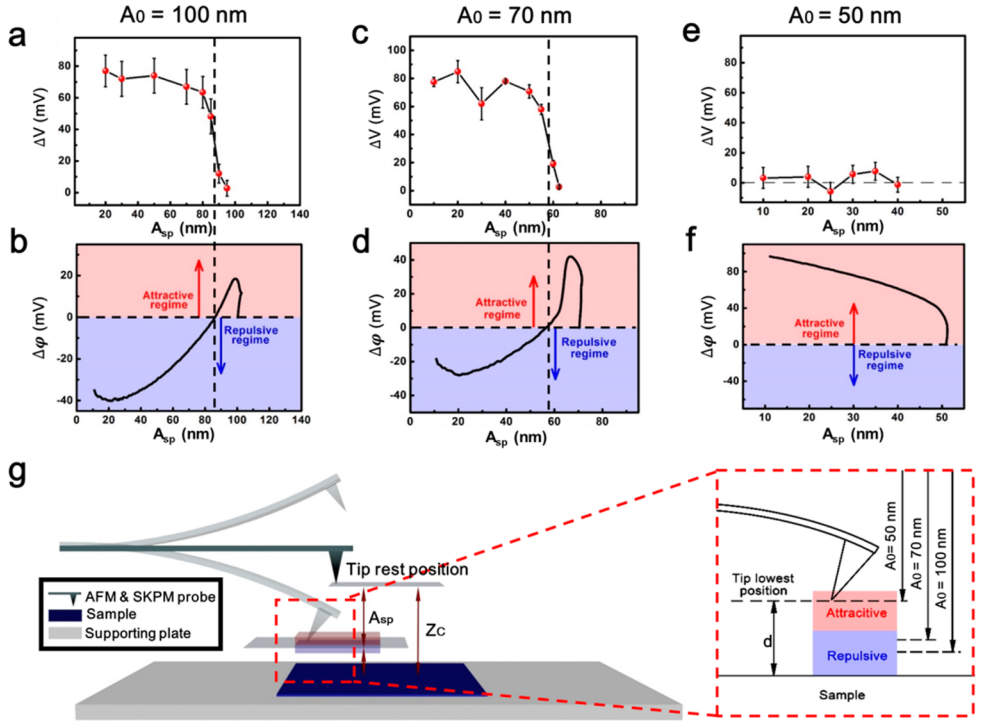

Figure 3. Experiment to explore the relationship between contact electrification and the phase shift. (a–f) ΔV–A_{sp} and $\Delta\varphi$–A_{sp} curves under the conditions of A_0 = 100, 70, and 50 nm. (g) Schematic of the tip–sample interaction force of tapping scans with different scanning parameters (A_0 and A_{sp}).

by measuring the phase shift and decouple it from the measurement by keeping the tip out of the repulsive regime. We also processed the experiments with different samples and KPFM probes, from which the influence of adhesion between tip and sample materials on the scanning parameters for contact electrification, as well as that of the cantilever spring constant of the KPFM probe, has been obtained. With these two relationships, we have proposed practical methods to rationally adjust the scanning parameters of the topography scan to exclude contact electrification in surface potential measurements. Therefore, our study has developed a practical approach for correctly measuring surface potential using KPFM, which is essential for electrical characterization techniques of materials and devices at the nanoscale.

RESULTS AND DISCUSSION

For the noncontact (tapping-mode) topography scan pass of the KPFM, amplitude modulation-atomic force microscopy (AM-AFM) was used. In the AM-AFM, the probe cantilever was excited near its resonance frequency (f_0), with free vibration amplitude (A_0) set before the tip engaged the surface of the sample and set-point scanning amplitude (A_{sp}) set as a feedback parameter to measure the topography of the sample surface after the engagement.[23−26] As shown in Figure 1b,c, we scanned the same region (~4 μm^2 in area and shown as topography images in Figure 1b,c) on the surface of a parylene C thin film (~300 nm in thickness with a grounded copper layer on the bottom) with a platinum-coated silicon KPFM probe (~82 kHz in resonance frequency and 1.5 N/m in spring constant). The A_0 values for the two experiments were 100 and 30 nm, and A_{sp} was set to be 60% of A_0. As demonstrated in the surface potential images of Figure 1b,c, with different parameters of the topography scan passes, surface potential measurement results have a difference of around 40 mV, which is in the same order of magnitude as the measured surface potential when we compare the work function of different materials or when we characterize the transfer properties of electronic devices. This indicates that the topography scanning process has posed a significant influence on the measured surface potential of the material. It is reasonable that, in the tapping-mode topography scans in either one or both experiments, there has been contact electrification between the tip and parylene C thin film and resulted tribocharges, which strongly affects the result of the surface potential measurement.

We used the two-time scanning method to semiquantitatively study the effect of contact electrification on the surface potential measurement (Figure 2a). In the first scan, we did the KPFM scan in a smaller region (~4 μm^2 in area) using the parameters (A_0 and A_{sp}) that are examined as follows. In the second time, we scanned a larger region (~16 μm^2 in area and with the scanning region of the first time in the middle) using the parameters (A_0 = 50 nm and A_{sp} = 30 nm) that would not cause contact electrification (which has been proven by the following results). By comparing the surface potential difference (ΔV) of the two regions, we could test whether the parameters chosen for the first KPFM scans would cause any contact electrification, as well as semiquantitatively study the influence the first KPFM measurements have on the surface potential measurement.[19,20]

We first did the two-time scanning experiments on parylene C thin film (~300 nm in thickness with a grounded copper layer on the bottom) with a platinum-coated silicon probe (~82 kHz resonance frequency and 1.5 N/m spring constant). In our experiments, three different A_0 values were set to be 100, 70, and 50 nm with several different A_{sp} for each A_0. The results are demonstrated in Figure 2b–d. With an A_0 of 100 or 70 nm, there is contact electrification when A_{sp} is smaller than certain

DOI: 10.1021/acsnano.5b07418
ACS Nano XXXX, XXX, XXX–XXX

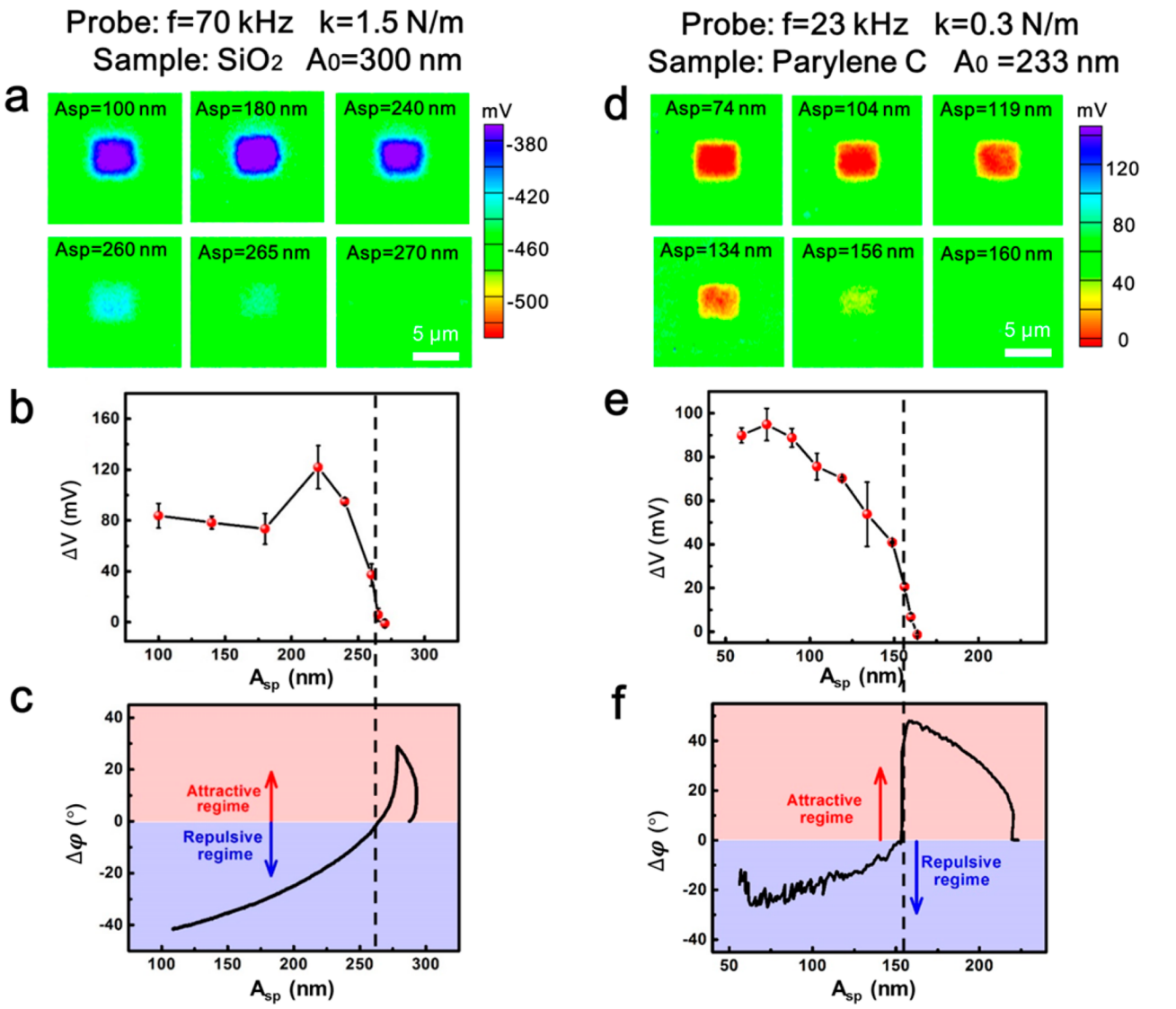

Figure 4. Relationships between contact electrification and phase shift of different samples and KPFM probes. (a–c) ΔV–A_{sp} and $\Delta\varphi$–A_{sp} curves of A_0 = 300 nm on the silicon oxide sample. (d–f) ΔV–A_{sp} and $\Delta\varphi$–A_{sp} curves of A_0 = 233 nm with the KPFM probe and cantilever spring constant k = 0.3 N/m.

values (95 nm for A_0 = 100 and 62.5 nm for A_0 = 70 nm). After contact electrification, the sample was negatively charged because of the effective work function difference between platinum and parylene C. For A_0 of 50 nm, there is no contact electrification observed. In order to quantify the contact electrification, we present the surface potential difference (ΔV) between the center (also the region of the first scan) and the edge (the rest of scanning region in the second scan) after the second KPFM scan (Figure 3a,c,e). According to the phase shift images in Figure 1b,c, there is an increase of the phase shift ($\Delta\varphi > 0$) for the scan with A_0 = 50 nm and A_{sp} = 30 nm, as well as a decrease of the phase shift ($\Delta\varphi < 0$) with A_0 = 70 nm and A_{sp} = 40 nm. Therefore, there might be a relationship between contact electrification and the change of the phase shift ($\Delta\varphi$). In order to acquire the change of the phase shift ($\Delta\varphi$) under different scanning parameters (A_0 and A_{sp}), we approached the probe tip to the surface of the sample in the tapping mode with different A_0 values (100, 70, and 50 nm) and obtained two relationships: one was between scanning amplitude (A_{sp}) and tip rest position (z_c) and the other one was between $\Delta\varphi$ and z_c (Figure S2a–c). Based on these two relationships, we present the $\Delta\varphi$–A_{sp} curves of different A_0 (Figure 3b,d,f). By comparing the ΔV–A_{sp} and $\Delta\varphi$–A_s curves of different A_f (100, 70, and 50 nm), we explored the relationship between contact electrification and the change of phase shift in the tapping mode. For the experiments of A_0 = 100 nm and A_0 = 70 nm, there are dramatic increases of ΔV from 0 (which means that contact electrification has had a significant influence on the surface potential) with A_{sp} being smaller than certain values (~95 nm for the experiment of A_0 = 100 and 62.5 nm for the experiment of A_0 = 70 nm), and these values correspond to the sign switch point of the $\Delta\varphi$ in the $\Delta\varphi$–A_{sp} curves. In the case of A_f = 50 nm, no contact electrification was observed. Also, there is no decrease in the phase shift under such circumstances. According to previous theories of the dynamics of a vibrating KPFM probe in the proximity of the sample,[29,30] the vibrating cantilever could be regarded as a harmonic oscillator with damping if there is no tip–sample interaction force. The phase shift is 90° if the driving frequency equals the resonance frequency. When the tip

DOI: 10.1021/acsnano.5b07418
ACS Nano XXXX, XXX, XXX–XXX

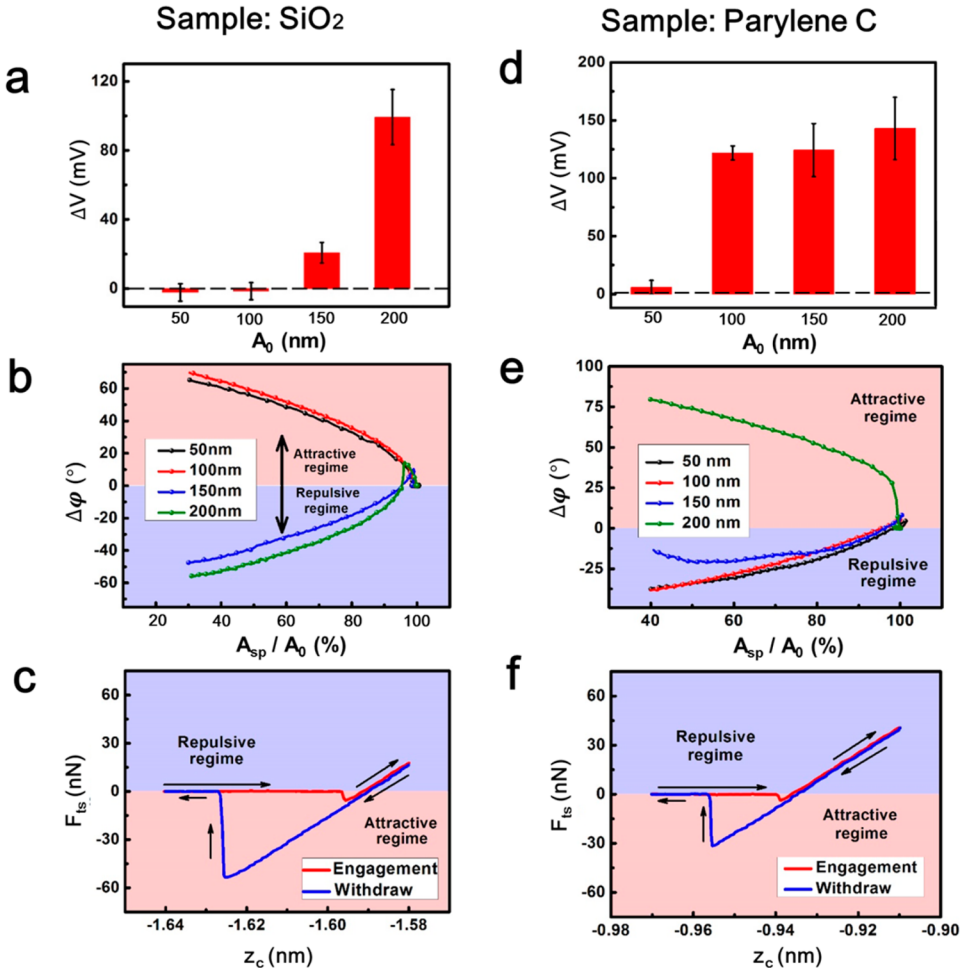

Figure 5. Relationship between the material of the sample and the scanning parameters for contact electrification. (a) Results of surface potential change caused by tapping scans with different A_0 (50, 100, 150, and 200 nm) on SiO_2. (b) $\Delta\varphi$–A_{sp} curves of different A_0 (50, 100, 150, and 200 nm) on SiO_2. (c) F_{ts}–z_c curves during the engagement and withdrawal of the probe tip on SiO_2 in the contact mode. (d) Results of surface potential change caused by tapping scans with different A_0 (50, 100, 150, and 200 nm) on parylene C. (e) $\Delta\varphi$–A_{sp} curves of different A_0 (50, 100, 150, and 200 nm) on parylene C. (f) F_{ts}–z_c curves during the engagement and withdrawal of the probe tip on parylene C in the contact mode.

has a net attractive force, it is in the attractive regime, and there is an increase of the phase shift ($\Delta\varphi > 0$). In contrast, if it has net repulsive force, it will be in the repulsive force regime, and there will be a decrease from the original phase shift ($\Delta\varphi < 0$). Therefore, the sign of $\Delta\varphi$ could be regarded as the symbol of the net tip–sample interaction force for each vibration cycle. According to this theory, the difference of contact electrification in the experiments with different A_0 (100, 70, and 50 nm) could be explained by the change of the tip–sample distance and the corresponding tunneling process. If the tip is in the attractive regime (A_0 = 50 nm), there is no electron transfer between the tip and sample through tunneling. By increasing the free amplitudes (A_0 = 70 and 100 nm), the probe cantilever can vibrate with more energy. In this way, it could overcome the repulsive force and enter the repulsive regime with certain A_{sp}, with the tip getting closer to the surface of the sample in its lowest position (as shown in Figure 3d,e). Because this tip–sample distance could result in tunneling, contact electrification is observed in scanning experiments with A_0 = 100 and 70 nm (Figure 3g). Moreover, knowing that the A_{sp} for the transition between the attractive regime and the repulsive force regime is exactly the same value for the drastic increase of ΔV from 0 (~95 nm for the experiment of A_0 = 100 and 62.5 nm for A_0 = 70 nm), the tunneling distance between the tip and the sample should be around the intermolecular distance, where the long-range attractive force equals the short-range repulsive force.

In order to use the relationship between ΔV and $\Delta\varphi$ to predict contact electrification in the tapping process, we have to confirm its feasibility among different KPFM probes and samples. Therefore, we also did experiments on silicon dioxide (SiO_2) samples (~300 nm in thickness) and experiments using the KPFM probe with a lower cantilever spring constant (k = 0.3 N/m) (Figure 4). For the experiment on SiO_2, we set the A_0 as 300 nm with different A_{sp}. From the ΔV–A_{sp} relationship (Figure 4a,b), there is contact electrification when A_{sp} is below 155 nm. By comparing this with the $\Delta\varphi$–A_{sp} relationship (Figure 4c), we could see that this is also the transition value between $\Delta\varphi > 0$ and $\Delta\varphi < 0$. In addition, the highest filled surface energy state of SiO_2 (sample) is above the Fermi level of platinum (tip). Therefore, electrons will transfer from the sample to the tip, leaving the contacted region in the first KPFM scan positively charged, which is in contrast with the results on parylene C.[20] The experimental results using the KPFM probe with lower cantilever spring constant are shown in Figure 4d–f. The A_f used in the experiment was 220 nm. The boundary A_{sp} (~155 nm) for contact electrification was

DOI: 10.1021/acsnano.5b07418
ACS Nano XXXX, XXX, XXX–XXX

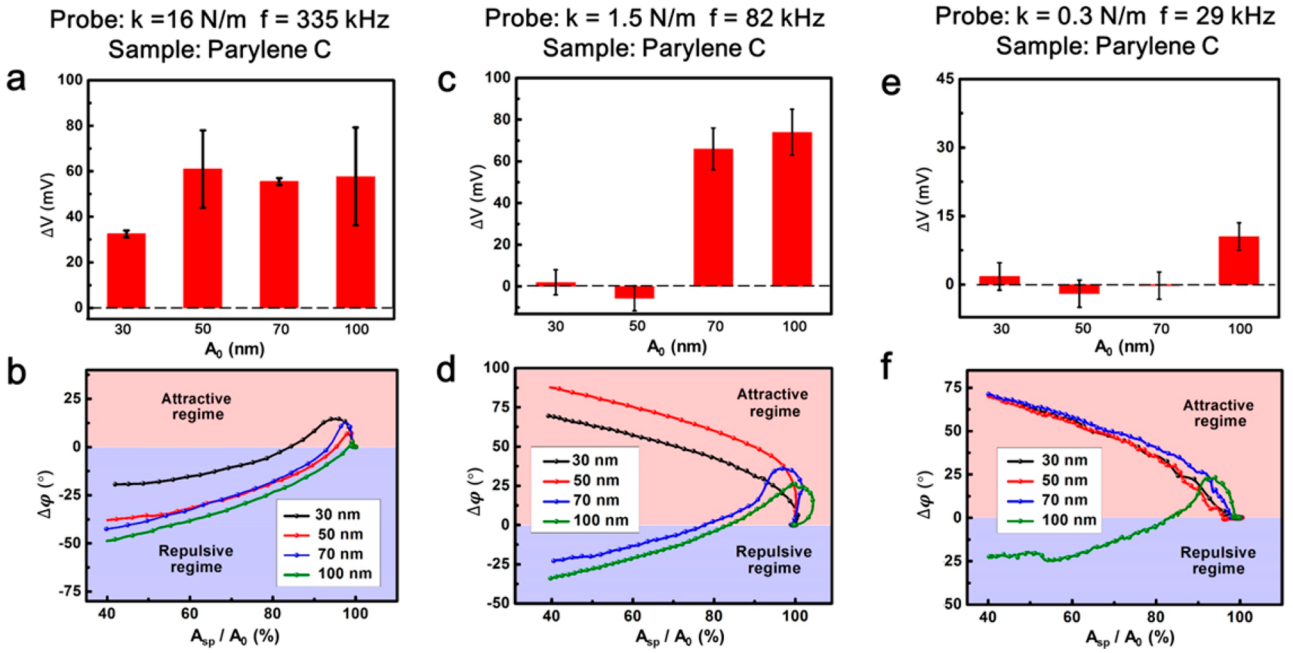

Figure 6. Relationship between the KPFM probe and the scanning parameters for contact electrification. (a,b) Results of surface potential change caused by tapping scans with different A_0 (30, 50, 70, and 100 nm) and the $\Delta\varphi$−A_{sp} curves of different A_0 (30, 50, 70, and 100 nm) using the KPFM probe with a spring constant of k = 16 N/m. (c,d) Results of surface potential change caused by tapping scans with different A_0 (30, 50, 70, and 100 nm) and the $\Delta\varphi$−A_{sp} curves of different A_0 (30, 50, 70, and 100 nm) using the KPFM probe with a spring constant of k = 1.5 N/m. (e,f) Results of surface potential change caused by tapping scans with different A_0 (30, 50, 70, and 100 nm) and the $\Delta\varphi$−A_{sp} curves of different A_0 (30, 50, 70, and 100 nm) using the KPFM probe with a spring constant of k = 0.3 N/m.

also the boundary for the sign change of $\Delta\varphi$. One more thing worth noting is that, unlike the smooth transition in previous $\Delta\varphi$−A_{sp} curves, there is the step-like transition in the $\Delta\varphi$−A_{sp} curve. That is because of the low spring constant of the probe cantilever, which is in accordance with previous works.[31−35] From the results of scanning experiments using different KPFM probes and samples, we can see that it is precise for us to predict whether there is contact electrification during the surface potential measurement by the change of the phase shift.

We also compared the experimental results of different A_f (50, 100, 150, and 200 nm) on different samples (SiO_2 and parylene C) (Figure 5). For all experiments, A_{sp} values were set to be 60% of A_0. For both materials, with the increase of A_0, the vibration energy of the cantilever gets larger. In this way, even if the ratio between A_{sp} and A_0 remains unchanged, the vibrating tip with a larger A_0 will have a larger decrease of phase shift, with a smaller tip−sample distance in the lowest position above the surface during the vibration. From the scanning experiment on SiO_2, we can see that there is no contact electrification until A_0 is increased to 150 nm (Figure 5a). Accordingly, there are only increases of phase shift in the curves for A_0 = 50 nm and A_0 = 100 nm, and decreases appear when A_0 reaches 150 and 200 nm (Figure 5b). In contrast, when it comes to the parylene C sample, the decrease of phase shift ($\Delta\varphi$ < 0) is first observed at smaller A_0 (A_0 = 100 nm) (Figure 5d), with the results of scanning experiments to prove that contact electrification can be observed in the conditions of A_0 = 100, 150, and 200 nm (Figure 5e). This distinction between different samples can be explained by the adhesion force between the tip and the sample. By comparing the relationships between the tip−sample interaction force (F_{ts}) and the z-axis position of the probe tip for different materials in the contact mode, the distinction in adhesion force of different materials could be demonstrated (Figure 5c,f). While the KPFM probe tip is approaching the surface of the sample, there will be the "jump-to-contact" in the force curve because the gradient of the tip−sample force is larger than the elastic constant of the cantilever. Similarly, there will be the "jump-off-contact" during the withdrawal of the probe tip because the cantilever elastic constant is greater than the gradient of tip−sample adhesive forces (F_{adh}). In general, the jump-off-contact distance is always greater than the jump-to-contact distance, so that the engagement trace and withdrawal trace do not coincide with each other, and there is a hysteresis loop.[36,37] For the same KPFM probe, a larger area of the hysteresis loop is caused by larger adhesion force (F_{adh}) and more work by the adhesion force (W_{adh}). In this way, by comparing the area of the hysteresis loops of SiO_2 and parylene C, we could see the difference in adhesion force of these two materials with same KPFM probe, that is, $F_{adh}(SiO_2) > F_{adh}$(parylene C). Therefore, it requires a larger free amplitude (A_0) for the probe tip to overcome adhesion force to enter into the repulsive regime on the SiO_2 sample.

Next, we present the effect of the KPFM probe on scanning parameters for contact electrification. In this section, we use three kinds of KPFM probes with different cantilever spring constants (k = 0.3, 1.5, and 16 N/m). We did the scanning experiments with four different A_f values (30, 50, 70, and 100 nm), and the A_{sp} values were set to be 60% of A_0. For the experiments of the KPFM probe with stiffest cantilever (k = 16 N/m), contact electrification was observed in the scans with all A_0 (Figure 6a), with $\Delta\varphi$ < 0 in the $\Delta\varphi$−A_{sp} curves for all A_0 (Figure 6b). When we decreased the cantilever spring constant of the KPFM probe (k = 1.5 N/m), contact electrification was not observed until A_0 = 70 nm (Figure 6c). In accordance, we can have $\Delta\varphi$ < 0 only in $\Delta\varphi$ < A_{sp} curves under the conditions

DOI: 10.1021/acsnano.5b07418
ACS Nano XXXX, XXX, XXX−XXX

of A_0 = 70 and 100 nm (Figure 6d). Continued decrease of the cantilever spring constant will further delay the contact electrification. For the KPFM probe with a cantilever spring constant of k = 0.3 N/m, only in the condition of A_f = 100 nm is there contact electrification (Figure 6e) and a decrease of $\Delta\varphi$ in the $\Delta\varphi-A_s$ curve (Figure 6f). The mechanism about how the cantilever spring constant of the probe affects contact electrification process lies in the elastic deformation of the cantilever. Suffering the interaction force when approaching the surface of the sample, a more compliant probe cantilever will have a larger elastic deformation, making it harder for the tip to enter the repulsive force regime for contact electrification.

Finally, we will discuss the methods to rationally exclude contact electrification from surface potential measurement for dual-pass KPFM. If there is already contact electrification during the measurement using KPFM, three practical methods can be utilized to eliminate the effect of contact electrification. The first one is to decease free amplitude (A_0). It has been proven that by vibrating with a small A_0, the probe tip may not enter into the repulsive region to have contact electrification. However, too small of a vibration amplitude may cause low scanning stability. Therefore, the decrease of A_0 should be within a rational range. The second one is to increase the set-point amplitude (A_{sp}) based on the $\Delta\varphi-A_{sp}$ curve of certain A_0. Based on the $\Delta\varphi-A_{sp}$ curve, we can adjust A_{sp} to make sure that the tip will not enter the repulsive regime. One possible concern with this method is that when A_{sp} is close to A_0, the topography scanning may also be unstable, which will largely affect the accuracy of the measurement. Under such circumstances, the choice of A_{sp} will be restricted to a narrow range. In this way, the adjustment could be regarded as supplementary to the change of A_f when there is not enough room for the modulation of A_f. The third one is to replace the KPFM probe with one that has a smaller cantilever spring constant. Actually, the above methods do not contradict each other to exclude contact electrification without affecting the accuracy of the measurement.

CONCLUSIONS

In this paper, we have proven the existence of contact electrification in the surface potential measurement of dual-pass KPFM for semiconductors and insulators, and some practical methods are demonstrated to rationally exclude it in the measurements. First, with the scan results using different parameters (A_0 and A_{sp}), we have demonstrated that contact electrification during the tapping topography scan would change the measured surface potential. Second, we have proven (with two-scan experiments of different probes and samples) that when the tip−sample distance is smaller than a certain value, there will be a significant surface potential change caused by contact electrification. This value can be around the sign switch point of the change of phase shift during the tapping vibration. Third, for different samples and probes, the scanning parameters that could cause contact electrification are not the same. When it comes to the sample that has a larger adhesion with the sample and probe with smaller cantilever spring constant, larger free amplitude is necessary for the probe tip to come into the repulsive region in order to have contact electrification. Finally, three practical ways to decouple contact electrification from the surface potential measurement of KPFM are proposed: decreasing the free amplitude, increasing the scanning amplitude, and replacing the KPFM probe into the one with a smaller cantilever spring constant.

METHODS

Equipment and Materials. The AFM system we used in this study was MFP-3D, manufactured by Asylum Research. The parylene C sample in the experiment was prepared by the deposition of a parylene C layer on the copper-coated silicon wafer using the SCS Labcoater PDS 2010. The thickness of the parylene C layer was controlled by the weight of the parylene C source and measured by SEM (SU8010 from Hitachi High-Tech) after deposition. The SiO_2 sample in the experiment was a commercial silicon wafer with wet thermal oxide by University Wafer, and the thickness of the oxide layer was measured by SEM (SU8010 from Hitachi High-Tech). The KPFM probes with a cantilever spring constant of 0.3, 1.5, and 16 N/m were PPP-CONTSCPt from Nanosensors, AC240TM-R3 from Olympus, and SSE_NCHR_13 from Nanotools.

Environmental and Experimental Parameters. The temperature was around 26.5 °C, and the relative humidity was 47% during the experiment. In the KPFM measurement of the probe with k = 0.3 N/m, the AC voltages were 78.11, 130.59, 181.49, and 256.86 mV for A_0 of 30, 50, 70, and 100 nm. For the probe with k = 1.5 N/m, those voltages are 24.24, 40.19, 56.26, and 80.07 mV. When it comes to the probe with k = 16 N/m, they are 15.87, 26.69, 37, and 54.21 mV. Between the two passes, the lift height of the probe tip was 50 nm.

Two-Time Experiment. In the first time, we scanned a 4 μm^2 region with the free amplitude (A_0) and set-point amplitude (A_{sp}) to examine 64 lines, and the scan rate was set to 0.5 Hz. The second time we scanned a 16 μm^2 region, with the scanning region used for the first time in the center, and the free amplitude (A_0) and scanning amplitude (A_{sp}) were set to 50 and 30 nm. We scanned for 64 lines with the scan rate of 0.5 Hz. We used the average value of the surface potential from a 4 μm^2 region as the result of the KPFM measurement.

$\Delta\varphi-A_{sp}$ Curves with Different A_0 in the Tapping Mode. These curves were obtained by the "single force" application of the MFP-3D AFM system in the tapping mode. The trigger points were set to be 40% of the free amplitudes. During the engagement and withdrawal of the probe tip, two channels were used to record the vibration amplitude and phase shift of the cantilever vibration with the tip rest position changing.

$F_{ts}-z_c$ Curves during the Engagement and Withdrawal of the Tip in the Contact Mode. These curves were obtained by the "single force" application of the MFP-3D AFM system in the contact mode. The maximum contact force between the tip and sample was 75 nN.

ASSOCIATED CONTENT

Supporting Information

The Supporting Information is available free of charge on the ACS Publications website at DOI: 10.1021/acsnano.5b07418.

Additional details and figures (PDF)

AUTHOR INFORMATION

Corresponding Author

*E-mail: zhong.wang@mse.gatech.edu.

Author Contributions

⊥S.L. and Y.Z. contributed equally.

Notes

The authors declare no competing financial interest.

ACKNOWLEDGMENTS

This research was supported by U.S. Department of Energy, Office of Basic Energy Sciences (Award DE-FG02-07ER46394), and the National Science Foundation (DMR-1505319).

DOI: 10.1021/acsnano.5b07418
ACS Nano XXXX, XXX, XXX−XXX

REFERENCES

(1) Binnig, G.; Quate, C. F.; Gerber, C. Atomic Force Microscope. *Phys. Rev. Lett.* **1986**, *56*, 930−934.
(2) Giessibl, F. J. Advances in Atomic Force Microscopy. *Rev. Mod. Phys.* **2003**, *75*, 949−983.
(3) Butt, H. J.; Cappella, B.; Kappl, M. Force Measurements with the Atomic Force Microscope: Technique, Interpretation and Aapplications. *Surf. Sci. Rep.* **2005**, *59*, 1−152.
(4) Falvo, M. R.; Clary, G. J.; Taylor, R. M.; Chi, V.; Brooks, F. P.; Washburn, S.; Superfine, R. Bending and Buckling of Carbon Nanotubes Under Large Strain. *Nature* **1997**, *389*, 582−584.
(5) Wang, Z. L.; Song, J. H. Piezoelectric Nanogenerators Based on Zinc Oxide Nanowire Arrays. *Science* **2006**, *312*, 242−246.
(6) García, R.; Knoll, A. W.; Riedo, E. Advanced Scanning Probe Lithography. *Nat. Nanotechnol.* **2014**, *9*, 577−587.
(7) Piner, R. D.; Zhu, J.; Xu, F.; Hong, S.; Mirkin, C. A. "Dip-Pen" Nanolithography. *Science* **1999**, *283*, 661−663.
(8) Lee, K. B.; Park, S. J.; Mirkin, C. A.; Smith, J. C. Protein Nanoarrays Generated by Dip-Pen Nanolithography. *Science* **2002**, *295*, 1702−1705.
(9) García, R.; Martinez, R. V.; Martinez, J. Nano-Chemistry and Scanning Probe Nanolithographies. *Chem. Soc. Rev.* **2006**, *35*, 29−38.
(10) Nonnenmacher, M.; o'Boyle, M. P.; Wickramasinghe, H. K. Kelvin Probe Force Microscopy. *Appl. Phys. Lett.* **1991**, *58*, 2921−2923.
(11) Jacobs, H. O.; Knapp, H. F.; Müller, S.; Stemmer, A. Surface Potential Mapping: A Qualitative Material Contrast in SPM. *Ultramicroscopy* **1997**, *69*, 39−49.
(12) Szwajca, A.; Wei, J.; Schukfeh, M. I.; Tornow, M. Self-Assembled Monolayers of Alkyl-Thiols on InAs: A Kelvin Probe Force Microscopy Study. *Surf. Sci.* **2015**, *633*, 53−59.
(13) Konig, T.; Simon, G. H.; Rust, H. P.; Heyde, M. Work Function Measurements of Thin Oxide Films on Metals-MgO on Ag (001). *J. Phys. Chem. C* **2009**, *113*, 11301−11305.
(14) Koley, G.; Spencer, M. G. Surface Potential Measurements on GaN and AlGaN/GaN Heterostructures by Scanning Kelvin Probe Microscopy. *J. Appl. Phys.* **2001**, *90*, 337−344.
(15) Bürgi, L.; Sirringhaus, H.; Friend, R. H. Noncontact Potentiometry of Polymer Field-Effect Transistors. *Appl. Phys. Lett.* **2002**, *80*, 2913−2915.
(16) Pingree, L. S.; Reid, O. G.; Ginger, D. S. Electrical Scanning Probe Microscopy on Active Organic Electronic Devices. *Adv. Mater.* **2009**, *21*, 19−28.
(17) Teague, L. C.; Hamadani, B. H.; Jurchescu, O. D.; Subramanian, S.; Anthony, J. E.; Jackson, T. N.; Richter, C. A.; Gundlach, D. J.; Kushmerick, J. G. Surface Potential Imaging of Solution Processable Acene-Based Thin Film Transistors. *Adv. Mater.* **2008**, *20*, 4513−4516.
(18) Luo, Y.; Gustavo, F.; Henry, J. Y.; Mathevet, F.; Lefloch, F.; Sanquer, M.; Rannou, P.; Grévin, B. Probing Local Electronic Transport at the Organic Single−Crystal/Dielectric Interface. *Adv. Mater.* **2007**, *19*, 2267−2273.
(19) Zhou, Y. S.; Liu, Y.; Zhu, G.; Lin, Z. H.; Pan, C.; Jing, Q.; Wang, Z. L. *In Situ* Quantitative Study of Nanoscale Triboelectrification and Patterning. *Nano Lett.* **2013**, *13*, 2771−2776.
(20) Zhou, Y. S.; Wang, S.; Yang, Y.; Zhu, G.; Niu, S.; Lin, Z. H.; Liu, Y.; Wang, Z. L. Manipulating Nanoscale Contact Electrification by an Applied Electric Field. *Nano Lett.* **2014**, *14*, 1567−1572.
(21) Mirkowska, M.; Kratzer, M.; Teichert, C.; Flachberger, H. Atomic Force Microscopy as a Tool to Explore Triboelectrostatic Phenomena in Mineral Processing. *Chem. Ing. Tech.* **2014**, *86*, 857−864.
(22) Charrier, D. S.; Kemerink, M.; Smalbrugge, B. E.; De Vries, T.; Janssen, R. A. Real *Versus* Measured Surface Potentials in Scanning Kelvin Probe Microscopy. *ACS Nano* **2008**, *2*, 622−626.
(23) Li, G.; Mao, B.; Lan, F.; Liu, L. Practical Aspects of Single-Pass Scan Kelvin Probe Force Microscopy. *Rev. Sci. Instrum.* **2012**, *83*, 113701.
(24) Albrecht, T. R.; Grütter, P.; Horne, D.; Rugar, D. Frequency Modulation Detection Using High-Q Cantilevers for Enhanced Force Microscope Sensitivity. *J. Appl. Phys.* **1991**, *69*, 668−673.
(25) Lü, J.; Delamarche, E.; Eng, L.; Bennewitz, R.; Meyer, E.; Güntherodt, H. J. Kelvin Probe Force Microscopy on Surfaces: Investigation of the Surface Potential of Self-Assembled Monolayers on Gold. *Langmuir* **1999**, *15*, 8184−8188.
(26) Ziegler, D.; Rychen, J.; Naujoks, N.; Stemmer, A. (2007). Compensating Electrostatic Forces by Single-Scan Kelvin Probe Force Microscopy. *Nanotechnology* **2007**, *18*, 225505.
(27) Guo, S.; Kalinin, S. V.; Jesse, S. Open-Loop Band Excitation Kelvin Probe Force Microscopy. *Nanotechnology* **2012**, *23*, 125704.
(28) Nonnenmacher, M.; o'Boyle, M. P.; Wickramasinghe, H. K. Kelvin Probe Force Microscopy. *Appl. Phys. Lett.* **1991**, *58*, 2921−2923.
(29) Jacobs, H. O.; Knapp, H. F.; Müller, S.; Stemmer, A. Surface Potential Mapping: A Qualitative Material Contrast in SPM. *Ultramicroscopy* **1997**, *69*, 39−49.
(30) Jacobs, H. O.; Knapp, H. F.; Stemmer, A. Practical Aspects of Kelvin Probe Force Microscopy. *Rev. Sci. Instrum.* **1999**, *70*, 1756−1760.
(31) Ziegler, D.; Stemmer, A. Force Gradient Sensitive Detection in Lift-Mode Kelvin Probe Force Microscopy. *Nanotechnology* **2011**, *22*, 075501.
(32) García, R.; Perez, R. Dynamic Atomic Force Microscopy Methods. *Surf. Sci. Rep.* **2002**, *47*, 197−301.
(33) García, R.; San Paulo, A. Attractive and Repulsive Tip-Sample Interaction Regimes in Tapping-Mode Atomic Force Microscopy. Relationship between Phase Shift and Energy Dissipation in Tapping-Mode Scanning Force Microscopy. *Phys. Rev. B: Condens. Matter Mater. Phys.* **1999**, *60*, 4961.
(34) Tamayo, J.; García, R. Relationship between Phase Shift and Energy Dissipation in Tapping-Mode Scanning Force Microscopy. *Appl. Phys. Lett.* **1998**, *73*, 2926−2928.
(35) Cleveland, J. P.; Anczykowski, B.; Schmid, A. E.; Elings, V. B. Energy Dissipation in Tapping-Mode Atomic Force Microscopy. *Appl. Phys. Lett.* **1998**, *72*, 2613−2615.
(36) Cappella, B.; Dietler, G. Force-Distance Curves by Atomic Force Microscopy. *Surf. Sci. Rep.* **1999**, *34*, 1−104.
(37) Johnson, K. L.; Greenwood, J. A. An Adhesion Map for the Contact of Elastic Spheres. *J. Colloid Interface Sci.* **1997**, *192*, 326−333.

DOI: 10.1021/acsnano.5b07418
ACS Nano XXXX, XXX, XXX−XXX